Searching for evidence of stellar cycles by using variations in flares rate

Author: Gerard Massip i Gil
*Facultat de Física, Universitat de Barcelona, Diagonal 645, 08028 Barcelona, Spain.**

Advisor: Octavi Fors Aldrich
Dept. de Física Quàntica i Astrofísica, Institut de Ciències del Cosmos (ICCUB), Universitat de Barcelona, IEEC-UB, Martí i Franquès 1, E-08028 Barcelona, Spain.

Abstract: In this work, evidence of stellar cycles is searched by analyzing variations in the rate of stellar flares. The focus is on two main sequence M-type stars plus an additional G-type target, all of them observed for 12-13 years by the Kepler and TESS missions. Each star's data was detrended, and a flare detection method was applied. Then, in order to assess the existence of stellar cycles their cumulative Flare Frequency Distribution (FFD) was computed, as well as their fractional luminosity evolution. The typical distinct regions of a cumulative FFD, including the FFD's turnoff point, were identified in the Kepler plots for all targets. On the TESS plots, such morphology was generally less apparent. The evolution of the fractional luminosity exhibited a decreasing trend of 0.4-0.5 decimal exponents throughout the entire timescale in those stars that showed evidence of activity cycles. The validity of such evidence claims is also discussed.

I. INTRODUCTION

A stellar flare is an activity transient event in which a star increases its brightness for a short amount of time, typically a few minutes. Although stellar flares are unpredictable, their occurrence rate remains constant on fully convective stars (M4-5 and colder stars), whereas it displays periodical variability on stars that employ both radiative and convective energy transport. This modulation in the flare rate is closely related to the stellar activity cycle. A solar-type activity cycle has an average length of approximately 10 years. Our own Sun, which is a main sequence G2 star, has an activity cycle spanning about 11 years. The currently ongoing Solar Cycle 25 is expected to peak sometime around July 2025.

The study of stellar activity cycles is highly relevant due to its implications for human life. Flaring events often coincide with Coronal Mass Ejections (CME), which can result in solar storms that pose a significant threat to human infrastructure. Historical incidents such as the Carrington Event in 1859 and the solar storm that affected Quebec in 1989 serve as notable examples.

In addition to that, stellar flares are a significant research area in the field of astrobiology. They are hypothesized to potentially act as catalysts for the origin of life, by providing the necessary energy for prebiotic chemistry to transition into living organisms [1].

In this work, a 12-13 year long baseline, formed by light curves from both the Kepler and TESS missions, is employed in order to look for evidence of these activity cycles whenever possible.

The Kepler and the TESS missions have both made a great contribution to the field of exoplanet research. Launched in 2009, the Kepler space telescope continuously observed a specific area of the sky located near the Cygnus and the Lyra constellations border until the end of its first mission in 2013. On the other hand, TESS is a successor to Kepler. Focusing on the brightest and closest stars, it surveys the entire sky. It was launched in 2018 and its mission is still ongoing. The continuous nature of both missions' observations has also made their data products ideal for other time-domain focused areas of research, with stellar activity variation being one of them.

This study has been performed on data recovered from fully convective, radiative-convective M-type stars, plus G-type stars, all of which are in their main sequence phase. [2, 3] have been used as a reference for the analysis, along with the Python code `flare_cycles`[1], available in [2].

In Section II, an outline of the criteria followed in the target selection process is provided, followed by an explanation of the preparation and analysis of the data used in this study. The results of such analysis are explored in Section III.

II. METHODOLOGY

A. Target selection

The selected samples for this study had to be flaring stars, both observed by the Kepler and the TESS missions. As of early 2023, the Kepler FOV had been observed (at least) in TESS' sectors 14, 15, 26, 54 and 55, each of them being a $24^{\text{o}}\times96^{\text{o}}$ area of the sky observed for an average of 27 days.

Thus, in order to locate potential candidate stars for the study, a cross-match of the Kepler catalog of stellar flares [4] was performed with all the TESS sectors that covered the Kepler field. To do this, the correspondence between each star's identification number in the Kepler

*Electronic address: gerardmassipgil@gmail.com

[1] `https://github.com/mscoggs/flare_cycles`

Input Catalog (KIC) and in the TESS Input Catalog (TIC) was established using `kic2tic`[2].

Furthermore, the number of detected flares in [4] had to be greater than 390, 70% of which had to be in the 68% completeness threshold. Those specific numbers were chosen taking [2, 3] as a reference. The resulting sample was then manually surveyed in the SIMBAD Astronomical Database[3] to check for each candidate's spectral type, thus reducing the list to main sequence M- and G-type stars.

The objects of interest in [2, 3] were obvious choices for the M-type stars, since the existence of literature to refer to was deemed useful. Further bibliographic investigation was also performed in order to discard those that presented evidence of binarity, so that the raw data did not include additional modulation cycles. This research was also complemented with visual inspection of all the light curves. The full list of studied targets is depicted in Table I.

TABLE I: List of studied targets with their KIC, TIC, spectral type, visual magnitude and mass. The first two stars are studied in [2, 3], respectively. The KIC 1225335 main sequence status is discussed in Subsection III C.

KIC	TIC	Type	m_V	Mass ($M_\odot$)
8507979	272272592	M3.0Ve	14.471 ± 0.086	0.407 ± 0.020
9726699	273589987	M4.0Ve	12.961 ± 0.188	0.241 ± 0.020
12253350	299029180	G1.5IV-V	10.350 ± 0.006	1.073 ± 0.131

B. Data preparation

The light curves from both the Kepler and TESS missions used in this study were retrieved from the Mikulski Archive for Space Telescopes (MAST), using the Lightkurve Python package [5].

The Kepler data spans a period of four years of continuous observation, divided in 18 quarters. Both long and short cadence Kepler data products are available. Long cadence data was used in this work, since it was accessible for all the studied targets. Each long-cadence light curve has a total exposure time of 1800 seconds.

While Kepler data is only available for a single calibration pipeline, there are four options available for TESS data, each one with its own cadence. The goal was for the data set to cover the longest baseline possible, so the TESS pipeline and cadence selection was done favoring the retrieval of the most recent data available. Furthermore, in the case of KIC 8507979, since it is so faint the QLP pipeline was specifically chosen, because it is intended to better work on the dimmest targets observed by TESS.

Once the data was downloaded, bad quality light curve data points were removed and the resulting light curves were saved in FITS format, using the Astropy Python package [6].

C. Cumulative Flare Frequency Distribution and Fractional Luminosity evolution

The Altaipony Python package [7] was used during the data analysis process. To detect flares in the light curves, each one had to be detrended first. This detrending was performed by applying a Savitzky-Golay filter [8]. In this method, a polynomial approximation is applied into a moving, fixed-size window. This window's size was a tunable parameter in the method's implementation, and its value was fixed through trial and error to 75 for what were deemed as optimal results.

Once the light curves were detrended, flares should appear as noticeable spikes in a flat curve, quantified in relative flux units. Each flare event has its own Equivalent Duration (ED), measured within its Full Width Half Maximum (FWHM). To detect them, Altaipony's flare detection method was used. The flare detection criteria in this method involved identifying flare candidates as data points that display positive deviations above the median quiescent flux, which had to exceed $N_1 = 3$ times the local scatter. The sum of the deviation and flux error had to be $N_2 = 2$ times greater than the local scatter, and a minimum of $N_3 = 3$ consecutive data points had to meet these conditions. Those default values could also be tweaked, but no change was observed upon variation during this part of the workflow.

It is important to note that this process is different from the one performed in [2, 3] to prepare the data, despite the fact that in both papers the data is also retrieved from MAST. This is because in these works, the data was prepared with the IDL based software suite `FBEYE`[4], which employed different detrending and detection algorithms and was originally designed to work with Kepler light curves.

Also, even though the data set spans more than 10 years of observations, there is a big gap between the Kepler and the TESS data coverage. In addition to that, there are occasional smaller gaps caused by different reasons, such as a periodic rotation performed by the Kepler space telescope at the end of each observation quarter to maintain the satellite's solar panels oriented towards the Sun. These gaps are accounted for in Altaipony's flare detection method, which first detects those gaps and then processes each data stretch separately.

The data analysis was performed by plotting the processed flare data in two different ways. The first plot consists of the cumulative Flare Frequency Distribution (FFD) for both the whole Kepler and TESS data coverage, as depicted in Fig. 3 in [3]. For this plot, the frequency with which flares sorted by their ED happened

[2] `https://github.com/jradavenport/kic2tic`
[3] `https://simbad.unistra.fr/simbad/`
[4] `https://github.com/jradavenport/FBEYE`

on each mission's data set is displayed. Then, a linear fit in the log-log space is performed for each mission. Stars without stellar activity cycles are expected to present similar values for the linear fit's slope of each mission, so different enough values for each mission's fit slope could be interpreted as evidence of a stellar activity cycle.

The second plot demonstrates the temporal evolution of the logarithm of the fractional luminosity for all the flares in every Kepler quarter/TESS sector, as in Fig. 1 in [2]. The fractional luminosity is defined as $\frac{L_{\rm Fl}}{L_{\rm Q}}$, where $L_{\rm Fl}$ is the luminosity for each flare event and $L_{\rm Q}$ stands for the quiescent luminosity. $L_{\rm Q}$ is subjected to instrumental variability, and has different values for the Kepler and TESS missions on each star (because of the different bandpass on each mission). The determination of those quantities is not trivial, and while $L_{\rm Q}$ is available for KIC 8507979 in `flare_cycles` (Kepler value only) and for KIC 9726699 in [3] (both Kepler and TESS values), computing the missing values for all the selected targets was beyond this project's scope. In order to compute the fractional luminosity for each Kepler quarter/TESS sector, the equivalence presented in [2] is used: $\frac{L_{\rm Fl}}{L_{\rm Q}} = \frac{ED_{\rm Sum}}{t_{\rm exp}}$, where $t_{\rm exp}$ stands for the total exposure time, and $ED_{\rm Sum}$ stands for the sum of the ED of every flare detected on a given Kepler quarter/TESS sector. Then, the logarithm of this division is calculated. Finally, a linear fit is performed on the resulting scatter plot.

A horizontal trend is to be expected for a star without any stellar activity cycle. It is worth noting, though, that in [2] the trend on this plot is analyzed by means of a fit performed using a Markov chain Monte Carlo (MCMC) implementation, while a simple linear fit was used in this work to that end.

III. RESULTS

A. KIC 8507979/TIC 272272592

The cumulative Kepler and TESS FFD plots for KIC 8507979 can be seen in Fig. 1. The Kepler cumulative FFD clearly depicts the 3 typical sections of an FFD plot. Each one has a different slope: the first section spans from the lowest ED values to ∼400s, while the second one extends from this point until ∼1500s. This last point is the FFD's turnoff point, beyond which the more energetic, less frequent superflares are depicted in the plot.

The TESS cumulative FFD depicts a much smaller number of flares. That can be explained by the shorter observation baseline of the TESS dataset, along with the fact that KIC 8507979 is the dimmest star studied in this work, as can be seen in Table I. This also results in a much shorter FFD plot, which does not feature any of the distinct regions explained for the Kepler FFD.

This star is not fully convective, and as stated in [2] a stellar activity cycle should be expected for it.

The slope for the resulting linear fits performed in each FFD is $a_{Kepler} = -0.55 \pm 0.01$ for the Kepler data and $a_{TESS} = -0.83 \pm 0.06$ for the TESS data. They are noticeably different, even considering the uncertainty range, so this disparity could be seen as evidence for the existence of a stellar activity cycle for this star. Given the fact that it is not a fully convective star, this result aligns with the expected results from [2].

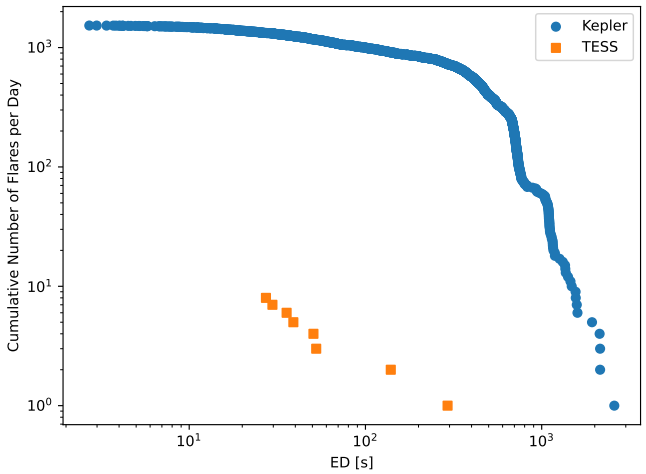

FIG. 1: Cumulative FFD plots from the whole Kepler and TESS data sets, for KIC 8507979.

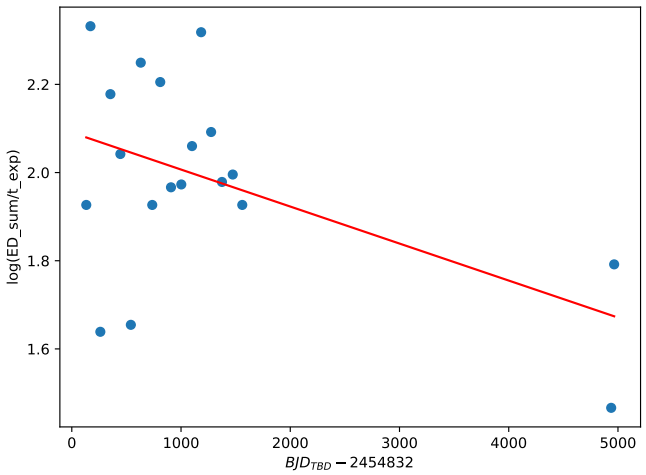

FIG. 2: Evolution of the fractional luminosity over the whole Kepler+TESS baseline for KIC 8507979. The origin of the time axis is in Kepler quarter zero, which corresponds to the Barycentric Julian Date (BJD) 2454832.

It is also worth noting the difference in the uncertainty magnitude between a_{Kepler} and a_{TESS}. As stated in [3], that is to be expected due to the shorter baseline of the observation in the TESS data set, along with its lower signal-to-noise ratio (SNR). The reason for this lower SNR can be found on Kepler's and TESS' different instrumental setup: the aperture of Kepler's telescope is larger than TESS', and in addition to that, they both use different filters. This variation in the magnitude of a_{Kepler} and a_{TESS} uncertainties is also found in the rest

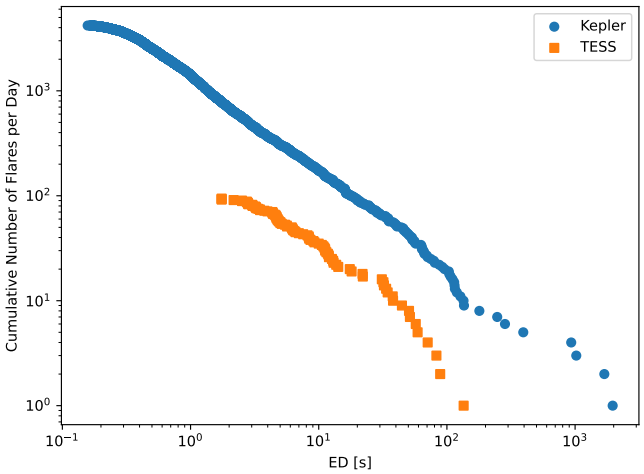

FIG. 3: Cumulative FFD plots from the whole Kepler and TESS data sets, for KIC 9726699.

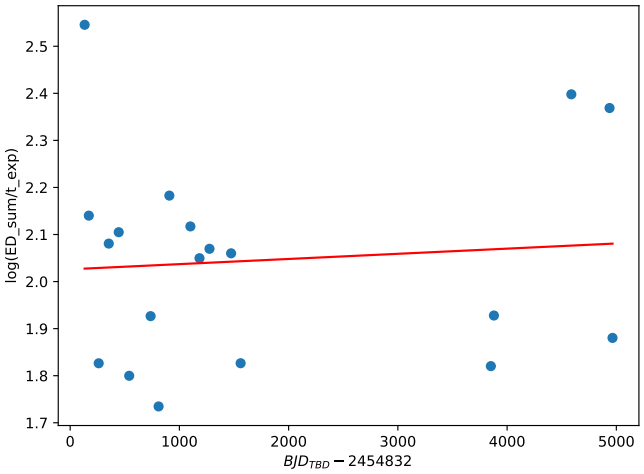

FIG. 4: Evolution of the fractional luminosity over the whole Kepler+TESS baseline for KIC 9726699. The origin of the time axis is in Kepler quarter zero, which corresponds to BJD=2454832.

of the studied targets.

As for the evolution of $\log\left(\frac{ED_{\rm Sum}}{t_{\rm exp}}\right)$ depicted in Fig. 2, it shows a noticeably decreasing trend of about 0.4 decimal exponents (dex) during the whole observation baseline, which supports the claim of a stellar activity cycle. However, it is worth noting that the values obtained for each data point in the Kepler data do not quite match those of [2].

B. KIC 9726699/TIC 273589987

The Kepler and TESS cumulative FFD plots for KIC 9726699 can be seen in Fig. 3. In this case, both plots present a rather linear trend. Also, once again the Kepler FFD distinctly features a turnoff point at an ED of ∼150s, while the presence of a turnoff point on the TESS plot is not clear at all.

In [3], it is stated that stellar activity cycles are expected in fully convective, slowly rotating stars. It is also stated that KIC 9726699 is rapidly rotating with a period of $P_{\rm rot} = 0.5925974$ days, so even though it is fully convective, no stellar activity cycle is expected.

The slope for the resulting linear fits performed in Fig. 3 is $a_{Kepler} = -0.869 \pm 0.001$ for the Kepler plot and $a_{TESS} = -0.893 \pm 0.020$. In this case, the values' high similarity is apparent, despite the fact that the uncertainty ranges do not quite overlap.

Even though the obtained values are not exactly the same as in [3], the absence of a stellar activity cycle could possibly be inferred from this analysis.

As for the evolution of $\log\left(\frac{ED_{\rm Sum}}{t_{\rm Exp}}\right)$ shown in Fig. 4, there is no significant upward or downward trend in the data, since there is only a variation of less than 0.1 dex during the whole observation baseline. The thesis of the absence of an activity cycle is therefore reinforced with these results.

C. KIC 1225335/TIC 229902918

It has been stated that all the stars studied in this work are in their main sequence phase. However, it can also be drawn from Table I that this star is in fact near the end of its main sequence phase, close to entering the subgiant branch. That is to be anticipated, since flaring in G-type stars is expected to happen precisely during the beginning and the end of their main sequence phase. The focus of this study is in the timescale of the modulation of the star's flare rate, and identifying how far it is from the main sequence goes beyond this project's scope.

There is no available literature to refer to in order to check whether KIC 1225335 should display an activity modulation cycle or not. Despite this fact, since it is a main sequence, not fully convective G-type star with a mass similar to the Sun (Table I), it can be claimed that evidence for a stellar activity cycle should be expected for this star.

The Kepler and TESS cumulative FFD plots for KIC 1225335 can be seen in Fig. 5. In this case, both the Kepler and the TESS plots clearly depict the typical FFD structure, with a turnoff point around ∼300s for the Kepler FFD and ∼125s for the TESS FFD. Both correspond to a Cumulative Number of Flares per Day of about 10 flares. The difference in the turnoff's ED for Kepler and TESS can also be explained by their instrumental setup and cadence.

The slope for the resulting linear fits performed in Fig. 5 is $a_{Kepler} = -0.71 \pm 0.01$ for the Kepler data and $a_{TESS} = -0.86 \pm 0.04$ for the TESS data. Just like with the results for KIC 8507979 shown in Section III A, they are noticeably different, even considering their uncertainty range, so this difference could be seen as evidence for the existence of a stellar activity cycle for KIC 1225335.

As for the evolution of $\log\left(\frac{ED_{\rm Sum}}{t_{\rm exp}}\right)$ depicted in Fig. 6,

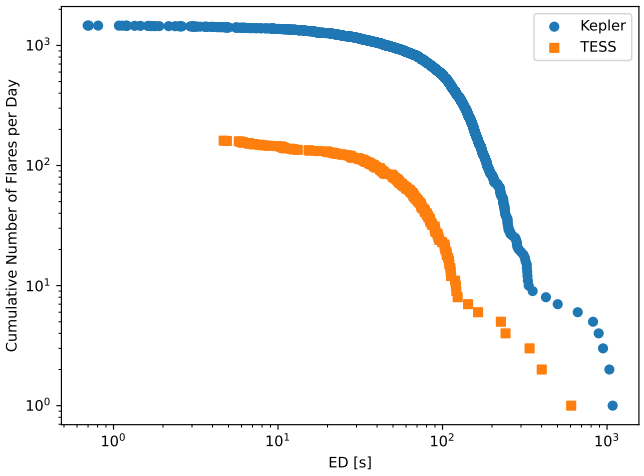

FIG. 5: Cumulative FFD plots from the whole Kepler and TESS data sets, for KIC 1225335.

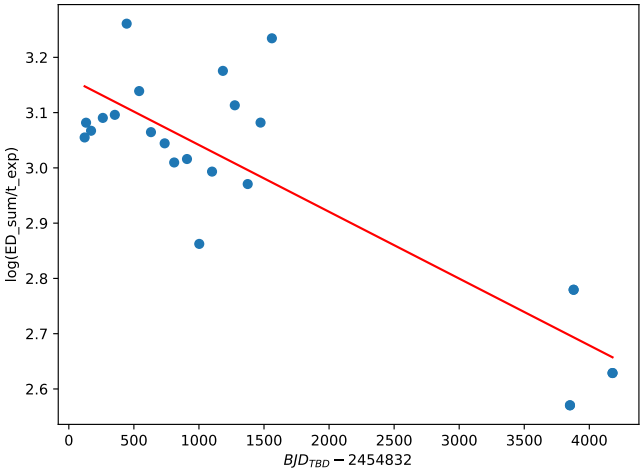

FIG. 6: Evolution of the fractional luminosity over the whole Kepler+TESS baseline for KIC 1225335. The origin of the time axis is in Kepler quarter zero, which corresponds to BJD=2454832.

it presents a noticeably decreasing trend of about 0.5 dex during the whole observation baseline, which supports the claim of a stellar activity cycle.

IV. CONCLUSIONS

Evidence for stellar activity cycles has been searched by looking for modulations in the flares rate of three different, main sequence stars.

Each star's data set combined information from both the Kepler and the TESS missions, forming a 12-13 year long timescale to look for such cycles. The light curves were detrended by means of a Savitzky-Golay filter, and flares were detected using Altaipony's flare detection method. Then, the evolution of the logarithm of each star's fractional luminosity was plotted, along with their cumulative FFD, splitting the data between the Kepler and the TESS light curves.

Both the fractional luminosity and the cumulative FFD plots pointed to the existence of a stellar activity cycle for KIC 8507979 and KIC 1225335. Since they are not fully convective stars, this aligns with the expected results.

On the other hand, the study for KIC 9726699 provided no solid evidence for any stellar activity cycle. Since such cycles should not be expected for rapidly rotating fully convective stars, this lack of evidence also aligns with the expected results.

As previously stated, the light curve detrending and flare detection methods used in this work have been different from those in the referenced literature. The obtained results may have been affected by that, probably leading to a somewhat different flare sample for each studied star than the one that would have been obtained using the original tools and methodology. This can explain why some obtained values, like the Kepler $\log\left(\frac{ED_{\text{Sum}}}{t_{\text{exp}}}\right)$ values for KIC 8507979 or the slopes for the linear fits performed in Fig. 3 for KIC 9726699, did not match with those available in the literature.

In addition, for the evolution of $\log\left(\frac{ED_{\text{Sum}}}{t_{\text{Exp}}}\right)$ plots, the difference in the methods chosen to fit the data also poses extra doubts on taking them as solid evidence for the presence (or lack) of stellar activity cycles.

This difference in the fit methodology has not been problematic in the case of the cumulative FFD plots, since a linear fit is also used in the original work.

Acknowledgments

I would like to thank my advisor Octavi Fors for all his insight and support during the last few months working in this project.

Additionally, I would like to express my gratitude to my parents for their unwavering support, not just during this project, but throughout this huge endeavor that has been becoming a Physicist.

[1] M. N. Günther et al., AJ **159**, 60 (2020), 1901.00443.
[2] M. T. Scoggins et al., RNAAS **3**, 137 (2019).
[3] J. R. A. Davenport et al., AJ **160**, 36 (2020), 2005.10281.
[4] J. R. A. Davenport, ApJ **829**, 23 (2016), 1607.03494.
[5] Lightkurve Collaboration et al., ASCL (2018), 1812.013.
[6] Astropy Collaboration et al., ApJ **935**, 167 (2022), 2206.14220.
[7] E. Ilin et al., A&A **645**, A42 (2021), 2010.05576.
[8] A. Savitzky and M. J. E. Golay, Anal. Chem. **36**, 1627 (1964).